Electronic Supplementary Information

Development of robust folded scaffold as fluorescence probes using butylidine linked Pyridazine based systems via aromatic π···π Stacking Interactions

Priyanka Yadav[a], Abhineet Verma[a], Vishal Prasad Sharma[a], Rashmi Singh[a], Tarun Yadav[b], Ranjeet Kumar[c],Shiv Pal[d] , Hariom Gupta[e] Satyen Saha[a], Ashish Kumar Tewari[a]

[a]Department of Chemistry, Institute of Science, Banaras Hindu University, Varanasi-221005
[b]Department of Physics, Institute of Science, Banaras Hindu University, Varanasi-221005
[c]Department of Chemistry, CMP Degree College, Prayagraj
[d]Department of Chemistry, IIT Bombay
[e]Phytochemistry Division, CSIR-Central Institute of Medicinal and Aromatics Plants (CSIR-CIMAP), Lucknow

Contents:

1. Experimental section

General methods

All reagents were purchased from commercial suppliers and used without further purification. Reactions were carried out at ambient temperature and were monitored by Thin layer chromatography (TLC) over Silica gel G UV active plates. Melting points of compounds were checked by Buchi melting point apparatus and uncorreceted.

Characterization

^{1}H and ^{13}C NMR spectra were recorded in $CDCl_3$ on JEOL AL500 FT-NMR spectrometer. Perkin Elmer Spectrum-2 FTIR spectrometer was employed for FT-IR data collection as KBr pellets in the region 4000 to 400 cm^{-1}. Raman study was done by Horiba LabRam HR evolution spectrometer. The sample was irradiated with the 633 nm output from a He\\Ne laser (30 mW, 1800 groves/mm grating, slit width 200 µm) and peltier cooled (-60 °C) CCD detector (model: Syncerity 356399, manufactured by Horiba Instrument Inc.) was used.

Photophysical properties

Steady-state UV-Visible spectra were measured by a spectrophotometer (CARY 100 BIO in the range of 200–800 nm), which has photometric linearity till an absorbance of 3.5 and wavelength resolution of 0.2 nm and attached with diffuse reflectance accessories (DRA) to measure solid state absorbance spectra. Fluorolog-3 spectrofluorometer (Model: FL3-11, Horiba Jobin Yvon was used for emission spectra measurement in solution and in solid state. The instrument is equipped with an integration sphere for measuring quantum yield in both solid and solution states.

X-ray Diffraction measurement

Crystal data were collected on a Bruker Kappa APEXII, CCD diffractometer using graphite monochromated Mo-Kα radiation (λ = 0.71073 Å) for compound 2CN and 1CN at 150 K. The structures were solved by direct methods and refined by full-matrix least squares on F using SHELX-2018. The powder X-ray diffraction (PXRD) data were recorded and collected on a Bruker D8-ADVANCE powder diffractometer with Cu Kα1 (λ = 1.5406 Å; power 1600 W, 40 kV, 40 mA) at a scan speed of five degree per minute.

Crystallographic data collection and structure refinement: Crystal data were collected on a Bruker Kappa APEXII, CCD diffractometer using graphite monochromated Mo-Kα radiation (λ = 0.71073 Å) for compound **2CN** and **1CN** at 150 K. The structures were solved by direct methods and refined by full-matrix least squares on F using SHELX-2018.[1] While non-hydrogen atoms were refined with anisotropic thermal parameters, all of the hydrogen atoms were geometrically fixed and were allowed to refine using a riding model. The refinements were converged to final values of R1 and wR2 0.059, 0.110 and 0.099, 0.104 respectively for **2CN** and **1CN**.The packing diagrams were generated using Mercury version 3.1.[2] PLATON was used for the analysis of bond lengths, bond angles, and other geometrical parameters.[3] Non-hydrogen atoms were refined anisotropically, and hydrogen atoms were geometrically fixed with thermal parameters equivalent to 1.2 times that of the atom to which they are bonded.

Computational methods: The theoretical calculations in order to obtain possible conformational structures of the compounds in gas phase were performed at well known DFT/B3LYP[4] level of theory available inGaussian09 software. The 6-311G**[5] basis set was used during complete computations. The self-consistent field (SCF) equation was solved iteratively to get the optimized geometries whose energies were found minimal on the potential energy surface.

Preparation of butylidine linked heteroaromatic systems:

Pyridazinone (3.6mmol) and potassium carbonate (7.32mmol) were dissolved in dry DMF and stirred for ~30 min followed by addition of 3-Chloro-2-chloromethyl-1-propene (10.98 mmol) and stirred for 24 h. Completion of the reaction was monitored via TLC. DMF was removed under reduced pressure through rotary evaporator and extracted with chloroform (200/200 x 3ml). The $CHCl_3$ layer was dried over anhydrous Na_2SO_4 and filtered. Chloroform was removed and the crude product was purified by column chromatography using ethylacetate and hexane (10:90) to get **CN** and (15: 85) to get **2CN** with yield of 0.32g (25%) and 1.46g (68%) respectively.

2-(2-(chloromethyl)allyl)-3-oxo-5,6-diphenyl-2,3-dihydropyridazine-4-carbonitrile (CN): M.P.: 112-116°C; Colourless solid; Yield: 0.32g(25%).^{1}H NMR (500 MHz,) δ 7.42 (t, *J* = 7.3 Hz, 1H), 7.36 (t, *J* = 7.4 Hz, 2H), 7.30 (t, *J* = 7.3 Hz, 1H), 7.22-7.18 (m, 4H), 7.08 (d, *J* = 7.6 Hz, 2H), 5.45 (s, 1H), 5.32 (s, 1H), 5.00 (s, 2H), 4.18 (s, 2H). ^{13}C NMR (125 MHz,) δ 156.6, 151.3, 146.0, 138.7, 134.1, 132.4, 130.6, 129.2, 129.0, 128.8, 128.3, 120.1, 114.0, 113.2, 54.6, 46.1, 24.8. Elemental analysis for $C_{38}H_{26}N_6O_2$: C, 69.71; H, 4.46; N, 11.61%; Found: C, 69.43; H, 4.17; N, 11.34%.

2,2'-(2-methylenepropane-1,3-diyl)bis(3-oxo-5,6-diphenyl-2,3-dihydro-pyridazine-4-carbonitrile) (2CN): M.P.: 142-148°C; Brown solid; Yield: 1.462g(68%). ^{1}H NMR (500 MHz,) δ 7.43 – 7.40(m, 2H), 7.36 (t, J = 7.5 Hz, 4H), 7.31 – 7.28 (m, 2H), 7.23-7.18 (m, 8H), 7.10 (d, J = 7.4 Hz, 4H), 5.45 (s, 2H), 5.03 (s, 4H).^{13}C NMR (125MHz, $CDCl_3$): δ 156.8, 151.4, 146.3, 137.0, 134.3, 132.5, 130.6, 129.3, 129.2, 129.1, 128.8, 128.3, 120.5, 114.0, 113.2, 55.0. Elemental analysis for $C_{38}H_{26}N_6O_2$: C, 76.24; H, 4.38; N, 14.04%; Found: C, 76.18; H, 4.14; N, 13.94%.

3-oxo-2-(2-((3-oxo-5,6-diphenyl-1,2,4-triazin-2(3H)-yl)methyl)allyl)-5,6-diphenyl-2,3–dihydro-pyridazine-4-carbonitrile (1CN): Methallyl linked heteroaromatic chloride **(CN)** (1.230 mmol) and Potassium carbonate (1.230 mmol) was dissolved in a minimum amount of dry DMF and stirred the mixture for 45 minutes at room temperature. Subsequently triazinone (1.23mmol) was added to the reaction mixture and stirring was continued for 24 h. Completion of the reaction was monitored by TLC. After completion of reaction, DMF was removed under vacuum and the reaction mixture was extracted with $CHCl_3/H_2O$ (200/200 × 3 ml). The $CHCl_3$ layer was over anhydrous Na_2SO_4 and filtered. Chloroform was removed and the crude product was purified by column chromatography using ethylacetate and hexane (18: 82) to get **1CN** with yield of 1.264g (80%).

. M.P: 188-192°C; Yellow solid; Yield:1.264g (80%) ; ^{1}H-NMR (500MHz, CDCl$_3$): δ 7.46 (d, *J* = 7.6 Hz, 2H), 7.41-7.36 (m, 4H), 7.33-7.28 (m, 6H), 7.25 (d, *J* = 7.9 Hz, 2H), 7.20 (t, *J* = 7.5 Hz, 2H), 7.13-7.09 (m, 4H), 5.48 (s, 2H), 5.05 (s, 2H), 5.00 (s, 2H); ^{13}C NMR (125MHz, CDCl$_3$): δ 166.8, 156.6, 153.1, 151.3, 146.1, 143.0, 136.5, 134.9, 134.2, 134.0, 132.4, 131.6, 130.4, 130.1, 129.4, 129.4, 129.1, 129.1, 129.0, 128.7, 128.6, 128.2, 128.2, 121.1, 113.8, 113.2, 55.6, 55.5. Elemental analysis for C$_{36}$H$_{26}$N$_6$O$_2$: C, 75.25; H, 4.56; N, 14.62%; Found: C, 75.14; H, 4.43; N, 14.58%.

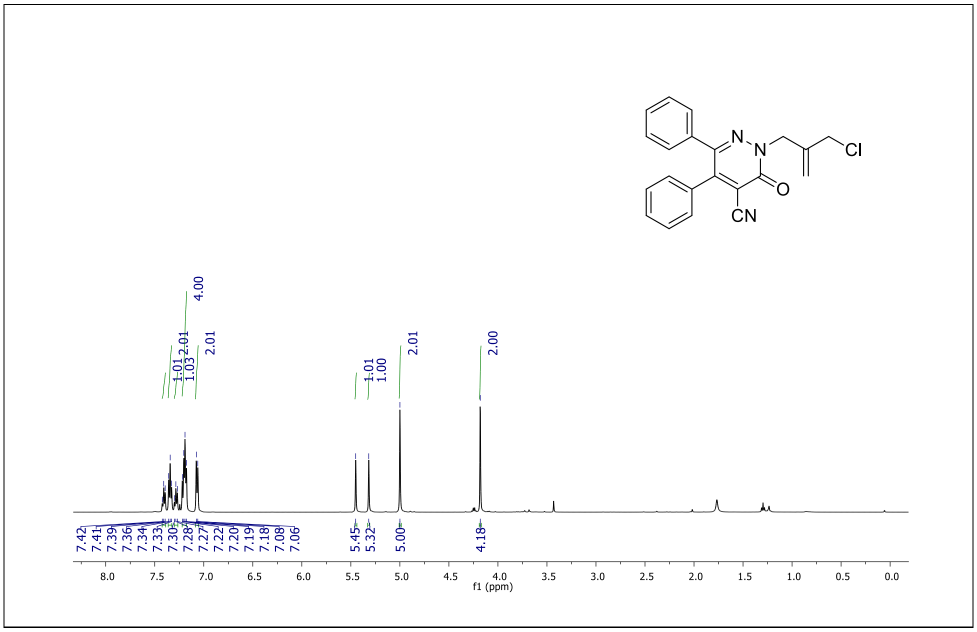

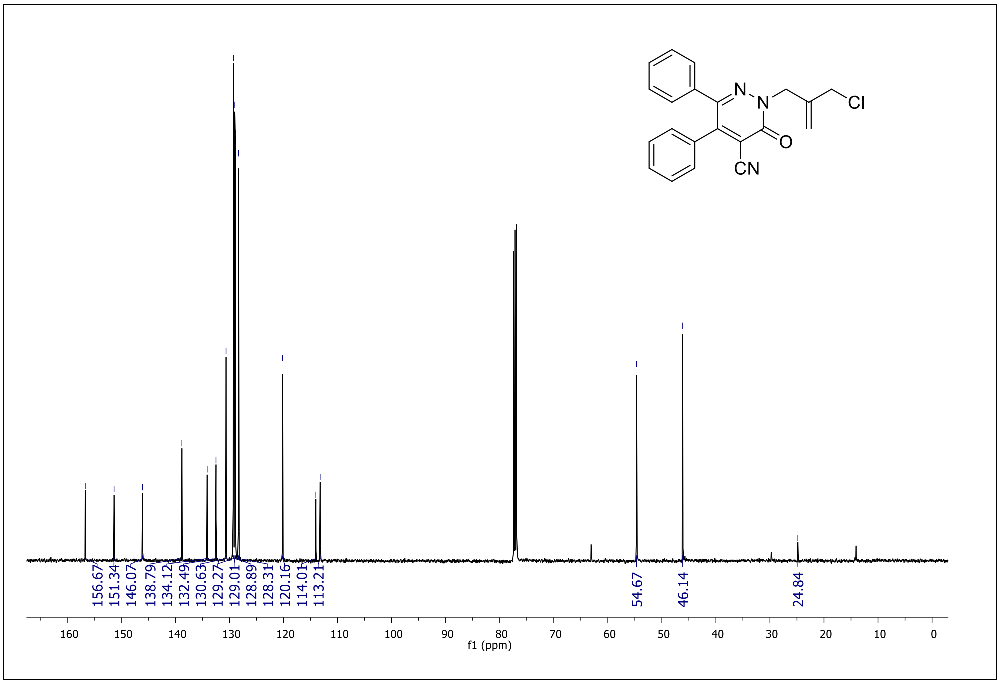

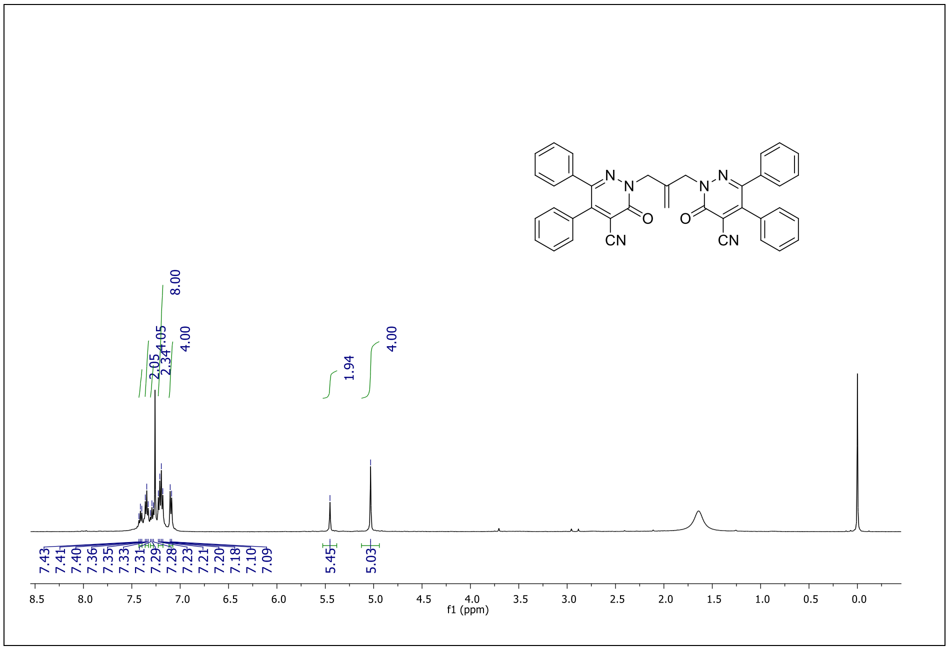
N
N
N
N
O
O
CN
CN
8.00
2.05
4.05
2.34
4.00
1.94
4.00
7.43
7.41
7.40
7.36
7.35
7.33
7.31
7.29
7.28
7.23
7.21
7.20
7.18
7.10
7.09
5.45
5.03
8.5
8.0
7.5
7.0
6.5
6.0
5.5
5.0
4.5
4.0
3.5
3.0
2.5
2.0
1.5
1.0
0.5
0.0
f1 (ppm)

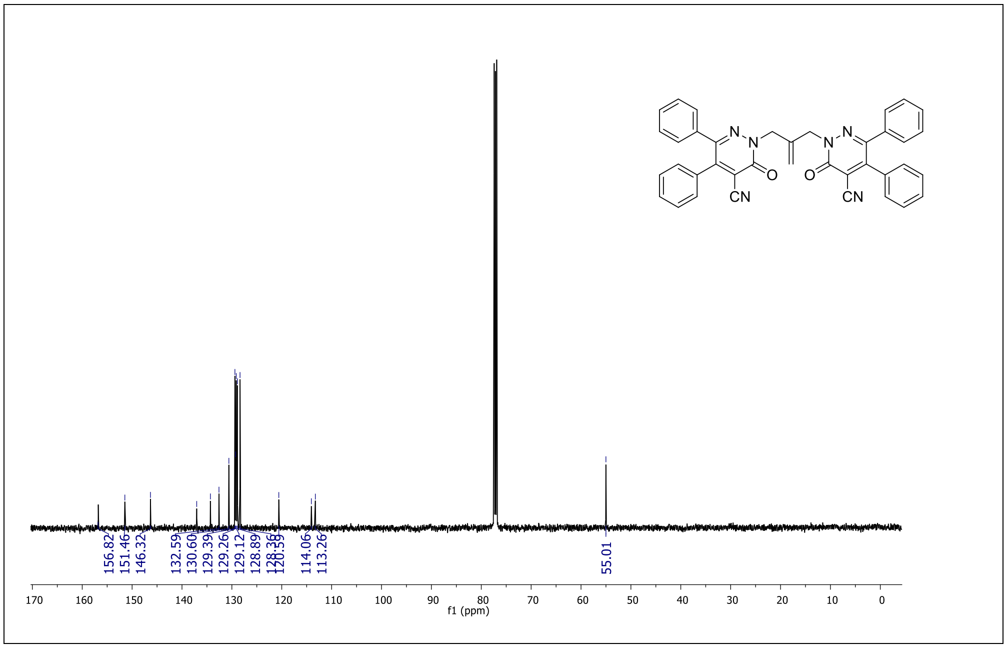
N
N
N
N
O
O
CN
CN
156.82
151.46
146.32
132.59
130.60
129.39
129.26
129.12
128.89
128.36
120.59
114.06
113.26
55.01
170
160
150
140
130
120
110
100
90
80
70
60
50
40
30
20
10
0
f1 (ppm)

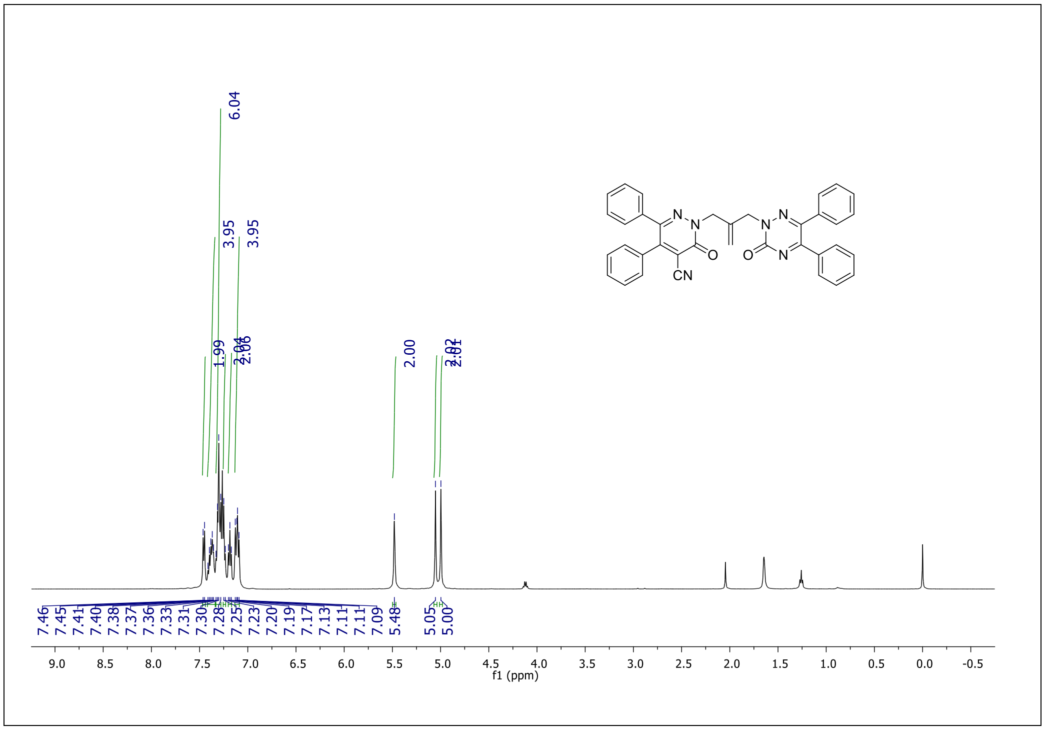
6.04
3.95
3.95
1.99
2.04
2.06
2.00
2.02
2.01
7.46
7.45
7.41
7.40
7.38
7.37
7.36
7.33
7.31
7.30
7.28
7.25
7.23
7.20
7.19
7.17
7.13
7.11
7.11
7.09
5.48
5.05
5.00
N
N
N
N
N
O
O
CN
9.0
8.5
8.0
7.5
7.0
6.5
6.0
5.5
5.0
4.5
4.0
3.5
3.0
2.5
2.0
1.5
1.0
0.5
0.0
-0.5
f1 (ppm)

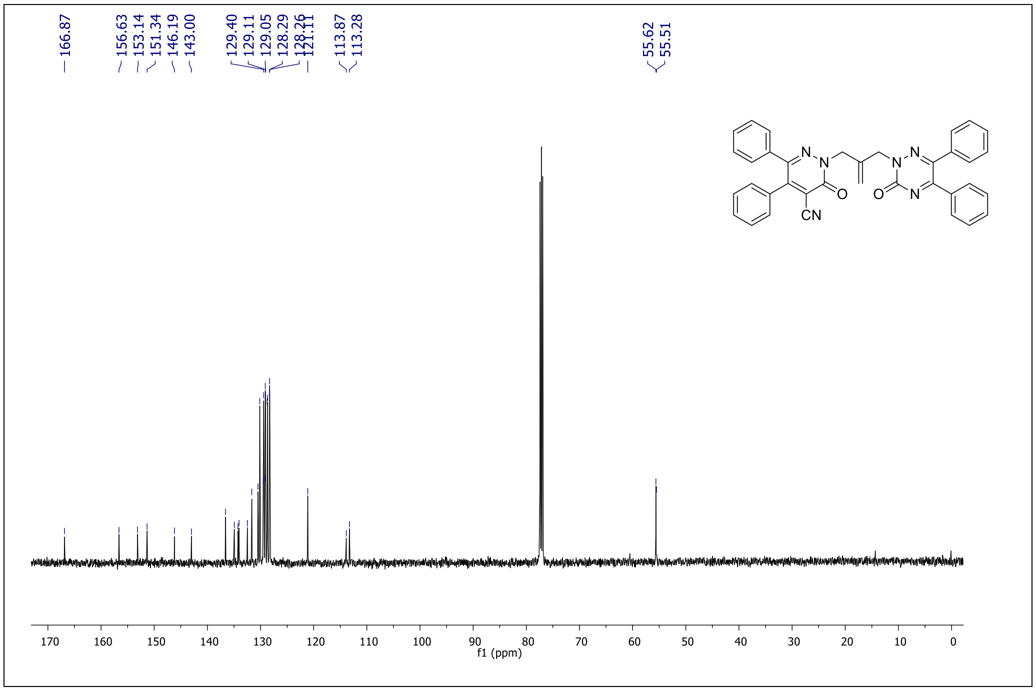
166.87
156.63
153.14
151.34
146.19
143.00
129.40
129.11
129.05
128.29
128.26
121.11
113.87
113.28
55.62
55.51
N
N
N
N
N
O
O
CN
170
160
150
140
130
120
110
100
90
80
70
60
50
40
30
20
10
0
f1 (ppm)

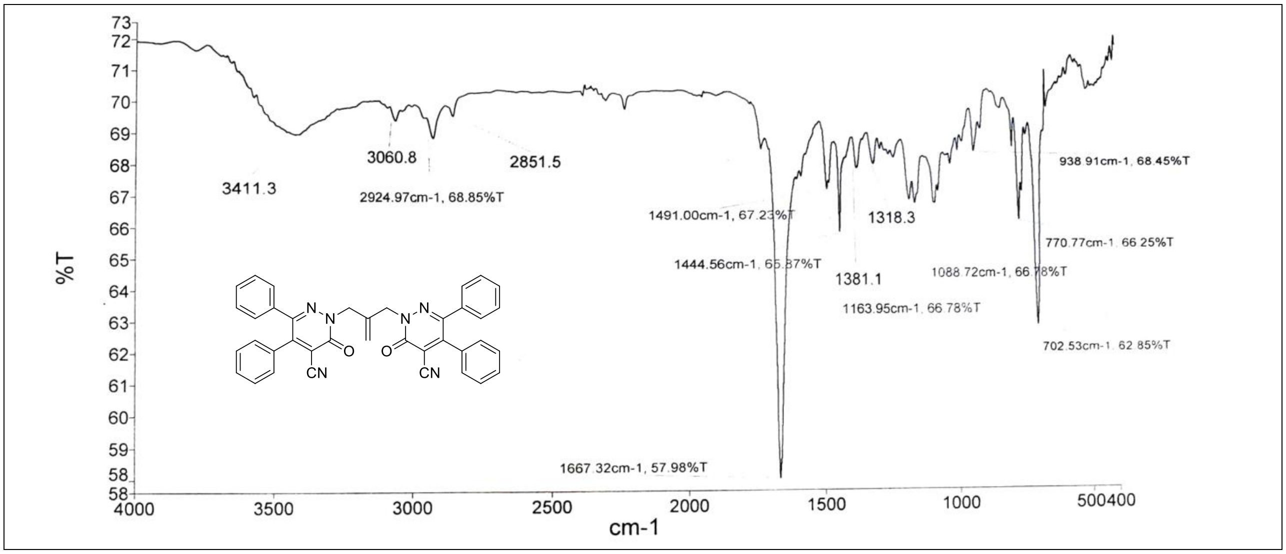

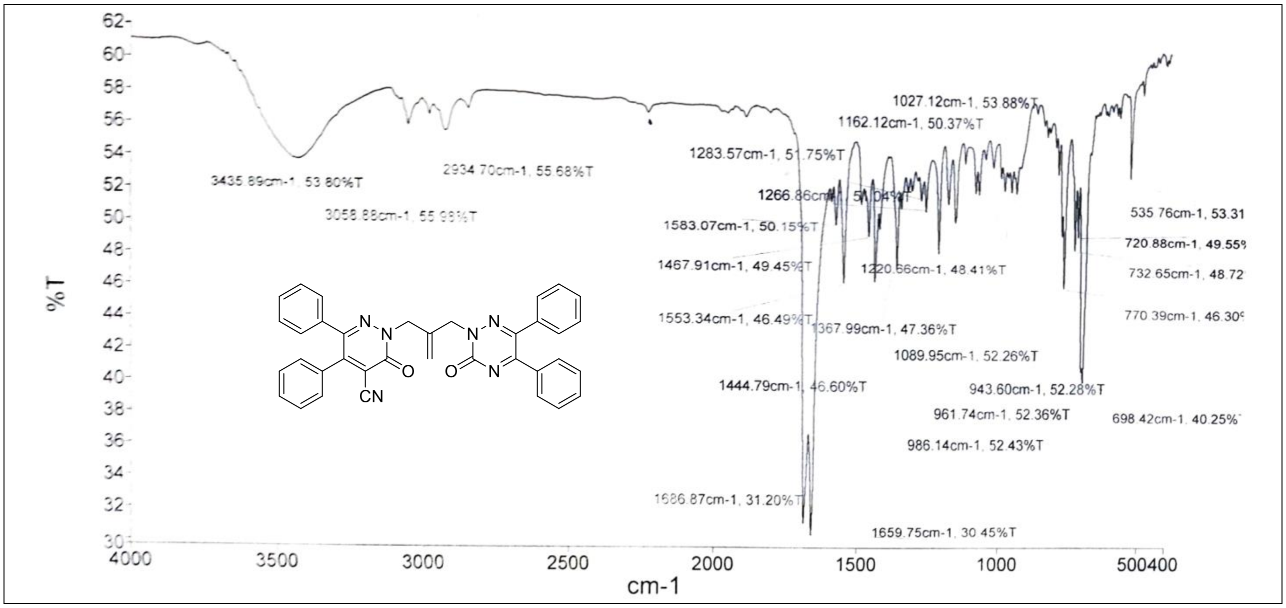

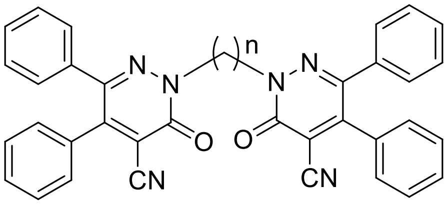	
(a)	(b)

Chart S1: Polymethylene linked pyridazinone and triazinone dimmers.

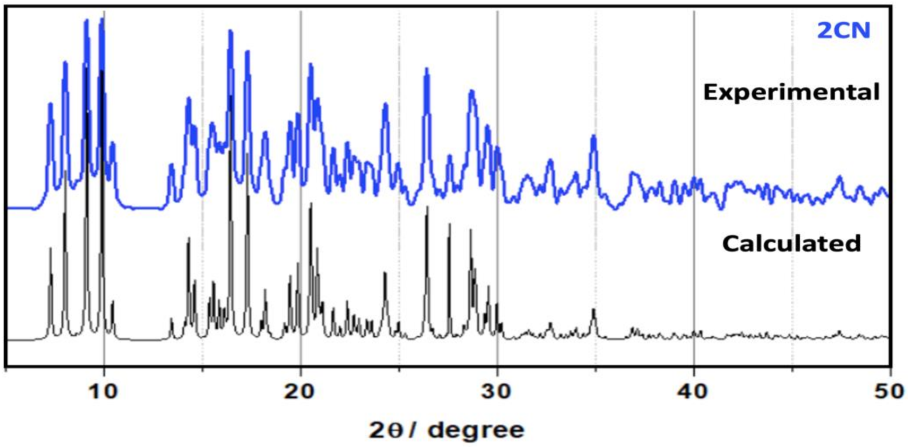

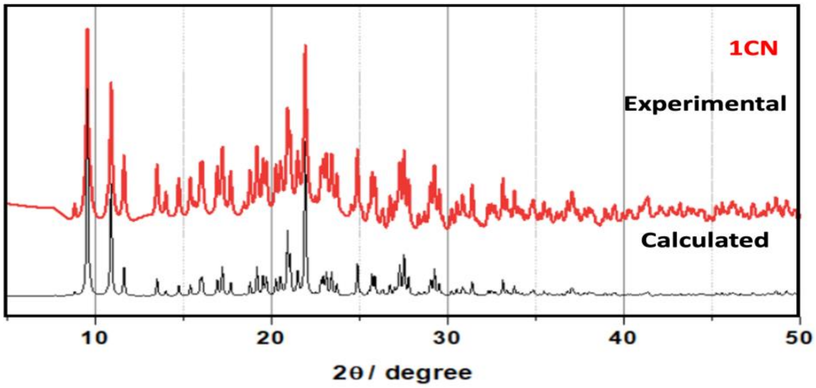

(b)

Figure S1: Powdered XRD pattern

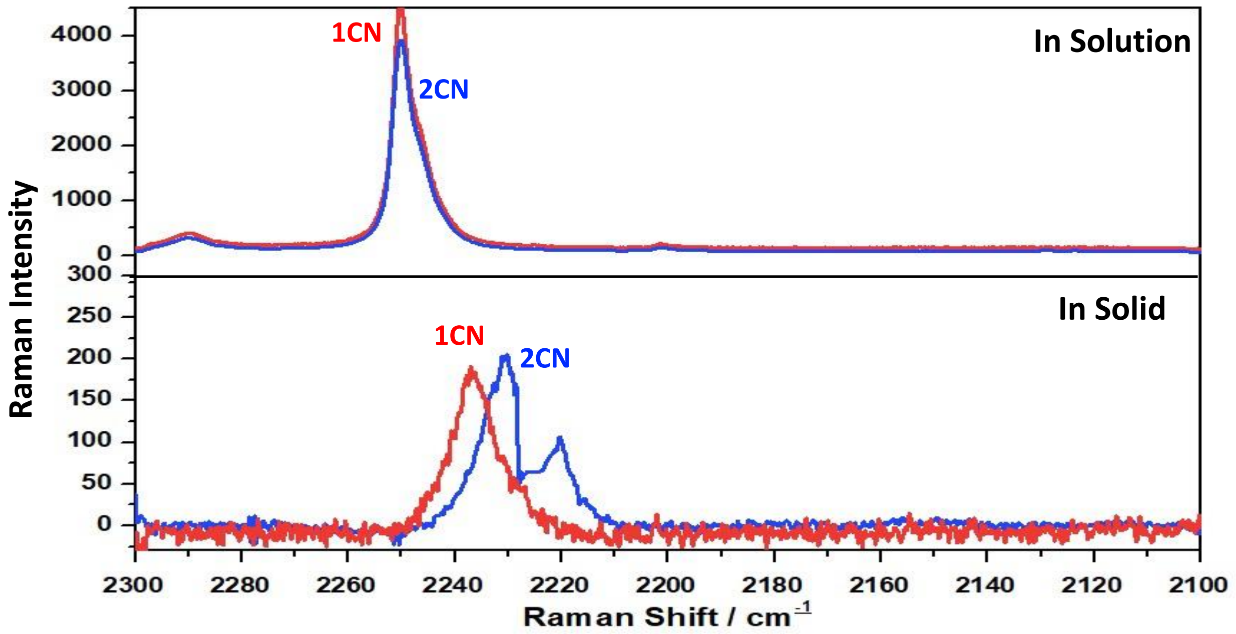

Figure S2: Raman spectrum showing the CN region presented in Solid and in solution phase.

Table S1: Representation of key bonds and angles showing intra-molecular interactions in their crystal structure and optimized structures at the DFT/B3LYP level of theory of compounds 2CN and 1CN.

S.No	D-H···A	Crystal structure			Optimized structure		
		H···A	D···A	D-H···A	H···A	D···A	D-H···A
		(Å)	(Å)	(°)	(Å)	(Å)	(°)
Compound 2CN							
1.	N1···N4	3.117			3.112		
2.	C(19)H···π(C20-N3centroid)	3.076	3.324	97.28	3.057	3.292	92.70
3.	C(37)H··· π(C20-N3centroid)	3.850	4.752	164.50	3.071	4.153	174.42
4.	C(37)H··· π(C38-N7centroid)	2.870	3.168	100.13	3.058	3.293	92.68

5.	C(21)H(21A)···O2	2.366	2.796	106.18	2.213	2.772	109.29
6.	C(3)H(3B)···O1	2.364	2.793	106.07	2.213	2.772	109.30
7.	C(21)H(21A)···N2	2.939	3.369	108.16	2.823	3.279	104.97
8.	C(3)H(3B)···N6	2.719	3.181	109.73	2.823	3.279	104.95
9.	C(3)H(3B)···π(pyridazinone centroid)	3.342	3.738	106.68	3.410	3.779	101.31
10.	C(21)H(21A)···π(pyridazinone centroid)	3.329	3.730	107.00	3.409	3.779	101.33
Compound 1CN							
1.	N1···N4	2.994			3.116		
2.	π···π(pyridazine-triazine centroid)	3.432			3.663		
3.	C(32)H···π(C20-N3centroid)	3.125	3.853	136.43	2.945	4.536	124.38
4.	C(26)H···π(C20-N3centroid)	3.464	3.901	111.46	3.683	4.127	106.66
5.	C(19)H···π(phenyl centroid)	3.081	3.501	109.41	3.728	4.007	96.95
6.	C(3)H(3A)···O1	2.385	2.804	105.42	2.243	2.788	108.45

Table S2: Intermolecular H-bond geometry parameters of compound 2CN and 1CN.

S.No	D-H···A	H···A(Å)	D···A(Å)	D-H···A(°)	Symmetry code
Compound 2CN					
1.	C(35)H···N3	2.626	3.321	131.98	-x,1-y,-z
2.	C(1)H(1B)···π(pyridazinone centroid)	3.820	4.620	145.90	
3.	C(16)H···π(phenyl centroid)	3.020	3.860	150.86	
4.	C(1)H(1B)···N2	2.719	3.581	154.57	1-x,1-y,1-z
5.	C(21)H(21B)···N3	2.747	3.529	138.18	-x,1-y,1-z
6.	C(1)H(1A)···π(phenyl centroid)	3.864	4.471	125.70	
7.	C(21)H(21B)···π(phenyl centroid)	3.780	4.191	108.60	
8.	C(33)H···O2	2.651	3.023	104.61	1-x,1-y,-z
Compound 1CN					
1.	C(15)H···π(phenyl centroid)	2.828	3.690	154.74	
2.	C(16)H···N3	2.636	3.386	138.14	-x,1-y,1-z

3.	C(1)H(1B) ···N3	2.613	3.475	154.36	-1+x,y,z
4.	C(13)H···π(pyridazinone centroid)	3.143	3.469	102.71	
5.	C(12)H···π(pyridazinone centroid)	3.293	3.545	98.02	
6.	C(21)H(21B)···O1	2.401	3.332	160.91	1-x,-y,1-z
7.	C(35)H···N5	2.668	3.298	125.59	-x,-1/2+y,1/2-z
8.	C(11) ···O2	2.594	3.401	145.40	1.5-x,-1/2+y,1/2-z
9.	C(29)H···π(phenyl centroid)	3.100	3.784	131.94	
10.	C(30)H···π(phenyl centroid)	3.382	3.931	120.09	

Table S3: Selected UV-vis absorption energy transitions at the TD-DFT/B3LYP level for 2CN and 1CN in acetonitrile.

Excited state	**λ_{ex}(nm)/(eV)**	**Oscillator strength (f)**	**Key transitions**
2CN			
S$_1$	384/3.2286	0.1267	H-1→L (17%), H→L (80%)
S$_2$	379/3.2685	0.0530	H-1→L (79%), H→L (18%)
S$_3$	363/3.4074	0.0178	H-2→L (3%), H→L+1 (93%)
S$_4$	361/3.4338	0.0278	H-2→L (8%), H-1→L+1 (86%)
S$_5$	343/3.6087	0.0114	H-3→L (13%), H-3→L+1 (11%), H-2→L (58%)
1CN			
S$_1$	395/3.1360	0.0449	H-1→L (2%), H→L (92%), H→L+1 (2%)
S$_2$	380/3.2620	0.0118	H-1→L (53%), H→L+1 (45%)
S$_4$	363/3.4063	0.0771	H-7→L+1 (3%), H-5→L+1 (3%), H-6→L+1 (2%), H-3→L+1 (2%) H-1→L+1 (82%)
S$_6$	352/3.5175	0.0076	H-3→L (3%), H-2→L (91%)

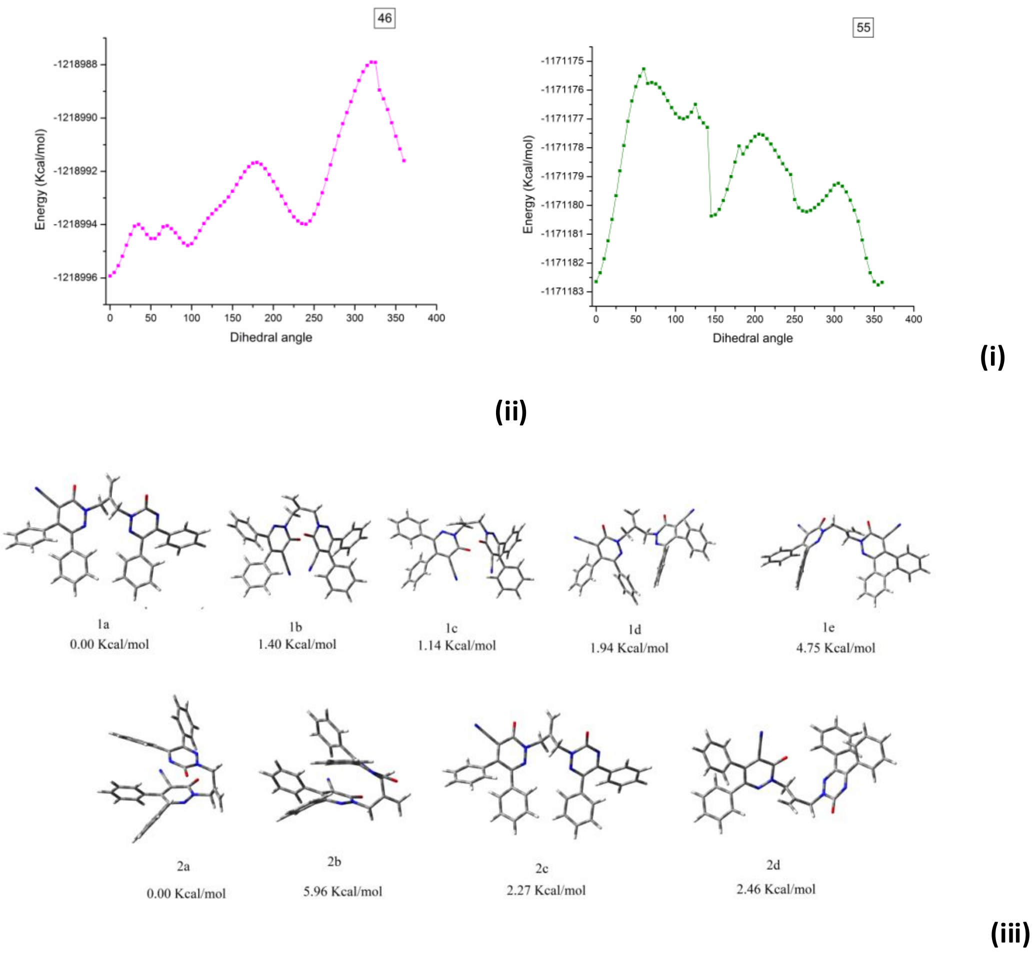

Figure S3: Representation of potential energy surface scans through linker dihedrals (scan (i) and (ii). (iii)Different possible conformers of compound 1CN and 2CN obtained by performing 1D potential energy scanning.

	Solid		Solution	
	Day light	UV-light	Day light	UV-light
Pyz				

2CN	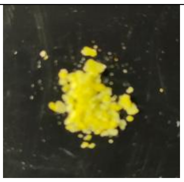	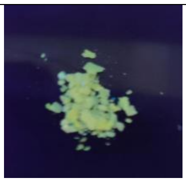	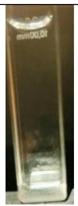	
Trz		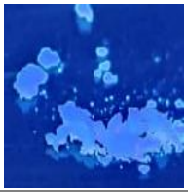		
1CN	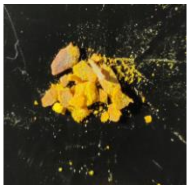	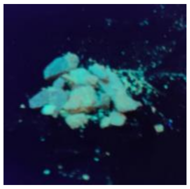		

Figure S4: Photos of the compounds in UV light and Day light.

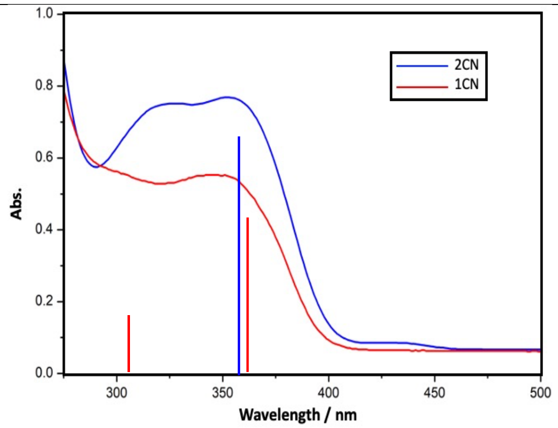

Fig S5: Comparison of experimental and calculated absorption spectra.

Table S4: Fingerprint plots and decomposed fingerprints showing various interactions ofcompounds 2CN and 1CN.

Interactions	Compound 2CN	Compound 1CN
Fingerprint	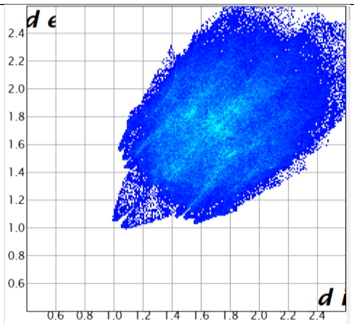	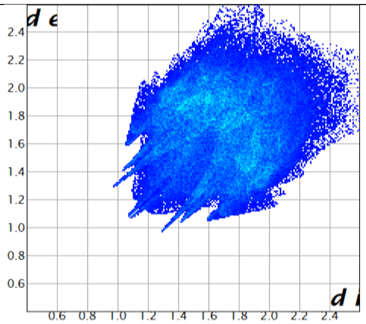
H···H	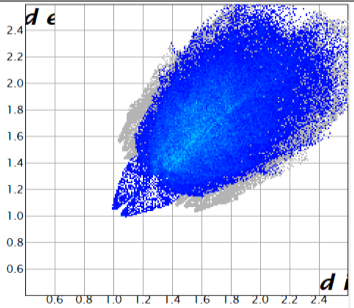	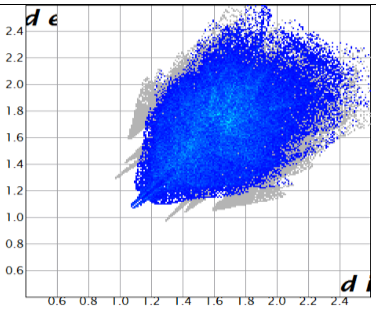
C···H	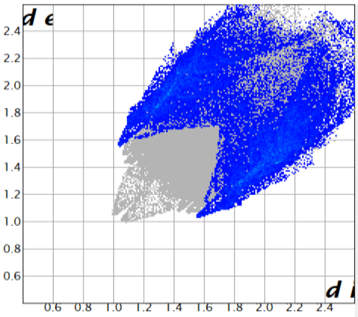	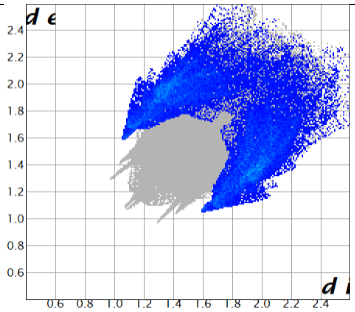
C···C	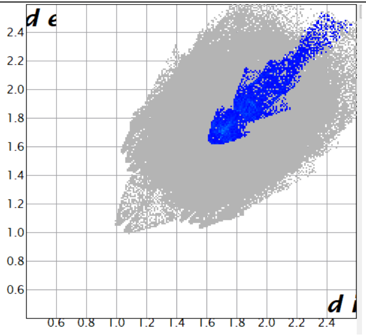	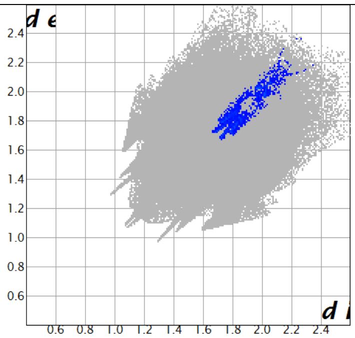

O···H	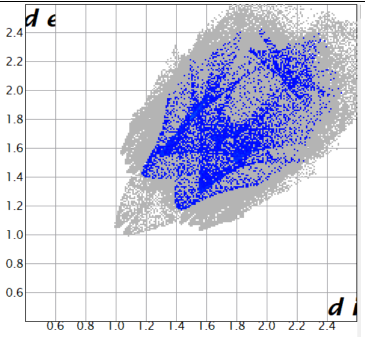	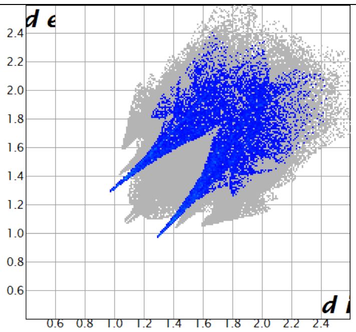
N···H	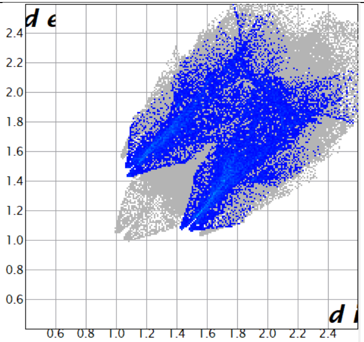	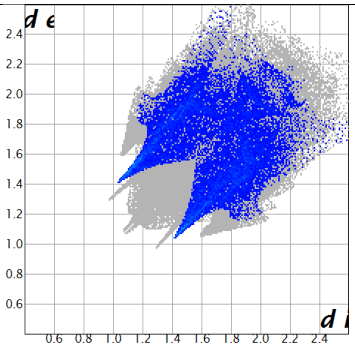

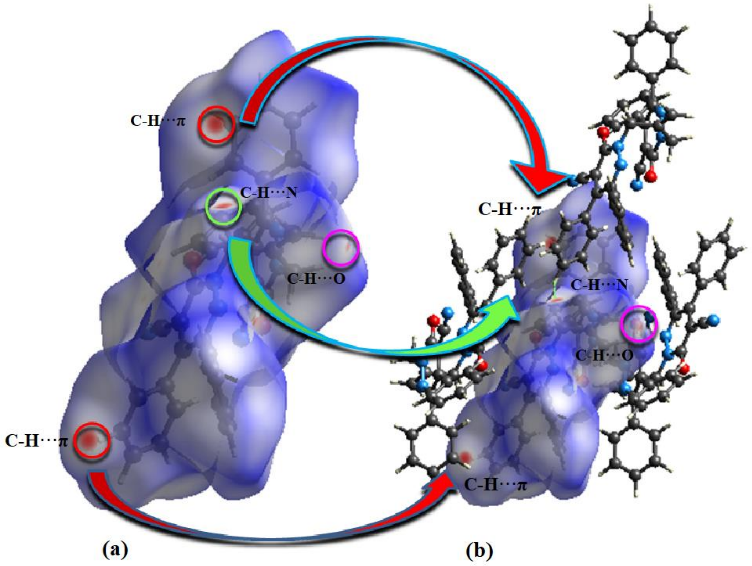

Figure S6:(a) Hirshfeld surfaces of 2CN mapped with d_{norm}(b) Hirshfeld surfaces surrounded with neighboring molecules exhibiting C-H···N, C-H···O and C-H···π interactions. Interacting sites have been shown via circled region.

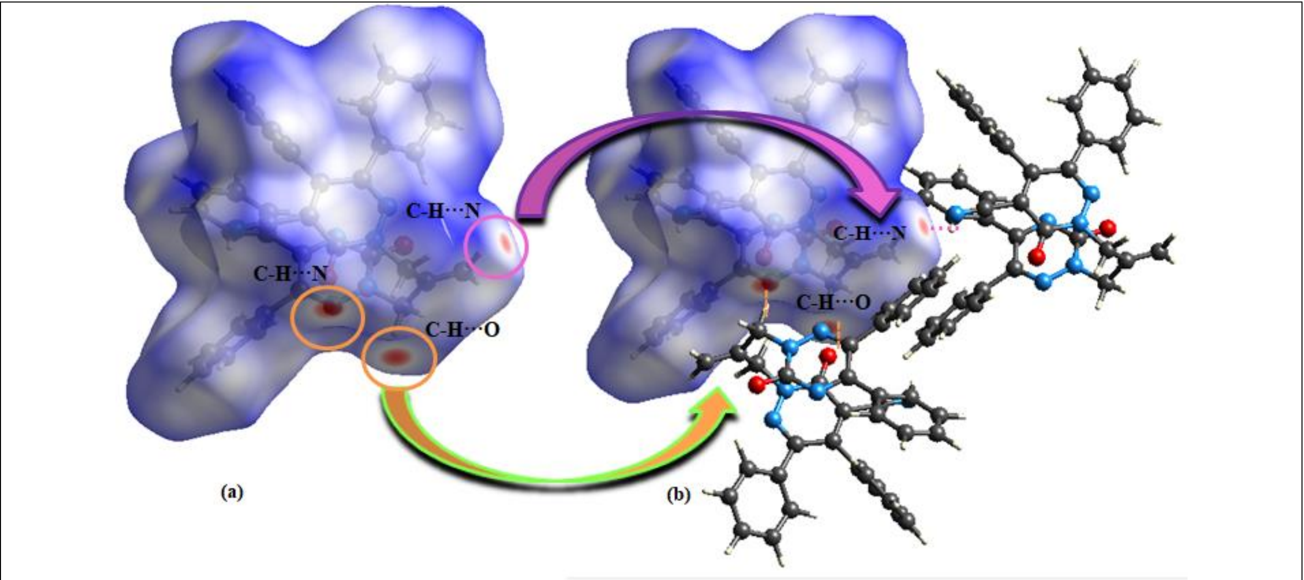

Figure S7: (a) Hirshfeld surfaces of 1CN mapped with d_{norm}(b) Hirshfeld surfaces surrounded with neighboring molecules exhibiting C-H···N and C-H···O and interactions. Interacting sites have been shown via circled region.

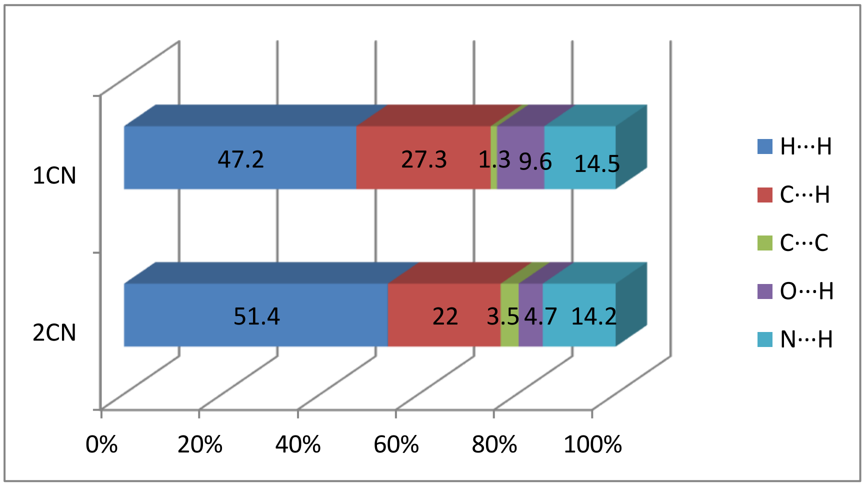

Figure S8: Bar graph for percentage contribution of various interactions.

References:

1. Sheldrick, G.; Acta Crystallogr. Sect. C: Structural Chemistry, 2015, 71, 3-8.
2. Macrae, C.; Bruno, I.; Chisholm, J.; Edgington, P.; McCabe, P.; Pidcock, E.; Rodriguez-Monge, L. ; Taylor, R. ; Streek, J. van de; Wood, P. J. Appl. Cryst., 2008, 41, 466-470.], ORTEP and OLEX II [Dolomanov, O.; Bourhis, L.; Gildea, R.; Howard, J.; Puschmann, H.; J. Appl. Crystallography, 2009, 42, 339-341.

3. (a) Spek, A.; J. Appl. Cryst., 2003, 36, 7-13. (b) Spek, A.; Utrecht University, Utrecht, The Netherlands 2008.

4. Frisch, M. J.; Trucks, G. W.;Schlegel, H. B. Scuseria, G. E.; Robb, M. A.; Cheeseman, J. R.;Scalmani, G.; Barone, V.; Petersson, G. A.;Nakatsuji, H.; Li, X.;Caricato, M.;Marenich, A. V.;Bloino, J.;Janesko, B. G.;Gomperts, R.;Mennucci, B.;Hratchian, H. P.; Ortiz, J. V.;Izmaylov, A. F.; Sonnenberg, J. L.; Williams-Young, D.; Ding, F.;Lipparini, F.;Egidi, F.; Goings, J.; Peng, B.;Petrone, A.; Henderson, T.; Ranasinghe, D.;Zakrzewski, V. G.; Gao, J.;Rega, N.; Zheng, G.; Liang, W.;Hada, M.;Ehara, M.;Toyota, K.; Fukuda, R.; Hasegawa, J.; Ishida, M.; Nakajima, T.; Honda, Y.; Kitao, O.;Nakai, H.;Vreven, T.;Throssell, K.; Montgomery, J. A.; Jr., Peralta, J. E.;Ogliaro, F.;Bearpark, M. J.;Heyd, J. J.; Brothers, E. N.;Kudin, K. N.;Staroverov, V. N.; Keith, T. A.; Kobayashi, R.; Normand, J.; Raghavachari, K.; Rendell, A. P.;Burant, J. C.; Iyengar, S. S.; Tomasi, J.;Cossi, M.;Millam, J. M.;Klene, M.; Adamo, C.;Cammi, R.;Ochterski, J. W.; Martin, R. L.;Morokuma, K.; Farkas, O.; Foresman, J. B.; Fox, D. J.; Gaussian, Inc., Wallingford CT, 2016.

5. (a) Becke, A.; J. Chem. Phy., 1993, 98, 5648-5652. (b) Lee, C.; Yang, W.; Parr, R.;Phys. Rev. B., 1988, 37, 785-789. (c) Vosko, S.; Wilk, L.; Nusair, M.; Canadian J. Physics, 1980, 58, 1200-1211. (d) Stephens, P.; Devlin, F.; Chabalowski, C.; Frisch, M.; J. Phy. Chem., 1994, 98, 11623-11627.